Engineering and Technology Journal
Journal homepage: https://etj.uotechnology.edu.iq

Evaluation of the synergistic effects of synthesized silver nanoparticles conjugated tetracycline

Nehia N. Hussein[a], Zahraa M. Zghair[a], Ruqaya J. Hussein[a], Alaa Z. Hameed[a], Amna M. Abdul-Jabbar [b], Buthenia A. Hasoon[a], Hamdoon A. Mohammed[c,d], Ghassan M. Sulaiman[a]*

[a] Division of Biotechnology, Department of Applied Sciences,University of Technology-Iraq, Alsina'a street, 10066 Baghdad, Iraq.
[b] Department of Anesthesia Technology, College of Health and Medical Technology, Uruk University, Baghdad, Iraq.
[c] Department of Medicinal Chemistry and Pharmacognosy, College of Pharmacy, Qassim University, Qassim 51452, Saudi Arabia.
[d] Department of Pharmacognosy and Medicinal Plants, Faculty of Pharmacy, Al-Azhar University, Cairo, Egypt.
*Corresponding author Email: ghassan.m.sulaiman@uotechnology.edu.iq

HIGHLIGHTS

- Antibiotic tetracycline was conjugated with silver nanoparticles
- The prepared nanoparticles and the antibiotic tetracycline formulation were characterized
- The formulation has good anti-bacterial and antioxidants potentials
- The formulation induced cytotoxicity against AMJ-13 cancer cells

ARTICLE INFO

Handling editor: Qusay F. Alsalhy

Keywords:
Antibiotics
Nanoparticles
Anti-bacterial activity
MIC
Pathogenic bacteria

ABSTRACT

The antibiotic impacts of classical drugs against bacteria could be enhanced via the conjugation of silver nanoparticles. After the successful coating of silver nanoparticles (AgNPs) with Tetracycline, the characterization of the conjugate properties was achieved through measurements with scanning electron microscopy (SEM) coupled to an energy-dispersive X-ray analyzer (EDX). The SEM analysis shows the appearance of silver nanoparticles with an average particle size of 22.82 nm and a cubic shape. Meanwhile, the EDX spectrum of silver NPs exhibits peaks corresponding to elemental silver. The anti-bacterial activity of pure Tetracycline and tetracycline-AgNP conjugates was examined against ten isolates of Pseudomonas aeruginosa. The tetracycline/AgNPs nanoparticles also strongly inhibited the growth of P. aeruginosa, as shown in experiments that involved the determination of the lowest inhibitory and lethal concentrations. It is noted that all of the isolates recorded the minimum inhibitory concentration at 60%, while the minimum inhibitory concentration for two isolates (1 and 10) was 100%. Genetically, higher frequencies of total chromosomal aberrations (TCAs) in blood cells were correlated with higher NP concentrations. The tetracycline-AgNPs effectively scavenged the 2,2-diphenyl-1-picrylhydrazyl (DPPH) free radicals. Toxicity tests against MCF-7 cancer cells revealed an antitumor effect of NPs against cancer cells, showing the capability of inhibiting the proliferation of cells and demonstrating highly significant effects.

1. Introduction

Tetracyclines (TC) comprise a widely spread family of naturally occurring compounds, among which chlortetracycline and oxytetracycline were the earliest to be described [1]. Excessive utilization of these compounds during the last decades has made many bacterial species resistant to their impacts [2]. Many prominent investigations were carried out to determine the capability of AgNPs to serve as vehicles to deliver various drug molecules to their exact targeted tissues, thereby enhancing their efficiency [3–5]. These attempts also successfully demonstrated the synergistic actions of these particles with antibiotic compounds [6,7]. Subsequent research was able to re-examine these findings, revealing the capability of these particles to successfully conjugate to several antibiotics, including Tetracycline, vancomycin, and the immunosuppressant azathioprine [8]. The strong activity of AgNPs against various types of microbes encouraged their progressive usage in applications that include, for example, wound dressings, catheters, and various domestic products [9]. Compounds with antibiotic properties proved crucial in various industries, including textiles, medicine, water disinfection, and food packaging. Nanoparticles possess antibiotic features that could be combined with those of classical drugs and overcome the problems caused by using

http://doi.org/10.30684/etj.2024.147316.1706
Received 29 February 2024; Received in revised form 28 March 2024; Accepted 30 March 2024; Available online 24 April 2024
2412-0758/University of Technology-Iraq, Baghdad, Iraq

organic materials, such as toxicity to life forms [10]. Research has highlighted that AgNPs exert their activities against microbes via several mechanisms of action. Via these mechanisms, these nanoparticles adhere to the bacterial cell wall and membrane, penetrate into the cytoplasm, cause damage to organelles, and induce reactive oxygen species (ROS) that induce cellular toxicity and oxidative stress [11,12]. Bacterial species resisting antibiotic treatment have raised growing concerns recently [13–15]. One species known as the main cause of urinary tract infections is the P. aeruginosa bacteria [16]. The advancement of nanotechnology as a credible, environmentally sustainable technique for producing a broad range of biocompatible materials and nanomaterials, including metal/metal oxide nanomaterials and nanocomposites, depends on developing eco-friendly green methods for producing nanoparticles. Green synthesis is therefore seen as an essential strategy to reduce the negative impacts associated with the traditional synthesis methods for nanoparticles routinely utilized in laboratories and industry [17]. This study aimed to develop a conjugation between Tetracycline and AgNPs and to enhance the latter's activity in treating this type of bacteria.

2. Materials and methods

2.1 Synthesis of the AgNPs

The chemical reduction method was used to prepare AgNPs. Silver nitrate (0.0849 g; Sigma-Aldrich, USA) was dissolved in 100 mL of deionized water. At 80°C, Trisodium Citrate Dihydrate (0.0103 g; Sigma-Aldrich, USA) and Sodium Dodecyl Sulfate (0.0144 g; Sigma-Aldrich, USA) were mixed in 100 mL of deionized water. The two mixtures were added dropwise over 30 minutes under continuous stirring, and the reaction was continued at 80°C for 4 hours. to ensure completion, which showed a yellow color. The produced AgNPs were cooled, collected in an amber bottle, and refrigerated [14,18].

2.2 AgNPs–Tetracycline Mixture

AgNPs (100 µg/mL) were mixed with Tetracycline (Sigma-Aldrich, USA) to a final 15 µg/mL concentration. A total of 0.2 mL of Tetracycline in 0.8 mL of AgNPs was mixed and well-homogenized on a stirrer, and the resultant solution was kept in the dark at room temperature [19].

2.3 Characterization of the conjugated AgNPs–Tetracycline

The conjugate of Tetracycline and AgNPs was characterized by SEM in addition to UV, FTIR, and XRD tests in the reference [20].

2.4 Bacterial isolates

Bacterial isolates of P. aeruginosa were obtained from the microbiology laboratory at Al Azizya Hospital, Wasit, Iraq. The isolates were directly transferred to the laboratory. The conventional methods to ensure their identity were based on microscopic examinations and were confirmed with the VITEK 2 system (VITEK, Biomérieux, Marcy-l'Etoile, France).

2.5 Determination of Minimum inhibitory concentration (MIC)

The MIC of the Tetracycline/AgNPs conjugate against each isolate was achieved using the macro-broth dilution method. Serial concentrations (10–90 µg/mL) were prepared in nutrient broth medium (NB; supplied by Hi-Media, India), followed by inoculation with bacterial cultured cells (10^6 cells, 0.2 µL). Tubes containing growth medium only were used as controls. The MIC represented the lowest conjugate concentration that caused growth inhibition in P. aeruginosa isolates [4].

2.6 Growth curve tests

AgNPs activity against the growth of pathogenic bacteria was determined according to [21]. A mixture involving AgNPs (0.1 mL) and (0.1 mL) from bacterial *suspension* was poured onto nutrient broth (10 mL), and 0.1 mL was distributed on a plate containing Mueller-Hinton agar, followed by incubation (37℃, 24 h) and then observation of viable bacterial cells after 0, 30, 60, and 90 min.

2.7 Chromosomal analysis

The experiment started with the addition of whole blood (0.5 mL) collected in a tube coated with heparin to RPMI-1640 medium (4.5 mL), including supplementations of 10% fetal bovine serum, a combination of penicillin and streptomycin, and 10 µg/mL of hemagglutinin (PHA). After incubation, the samples were left at room temperature until completely dried. The preparation slides were subjected to staining with Giemsa stain (2.5 min). Calculations of MI and BI values were made utilizing 1000 cells, whereas those of TCAs were achieved utilizing 25 wells of mitotic cells [22].

2.8 DPPH (1, 1-Diphenyl-2-picryl-hydrazyl) Assay

The pure AgNPs and the conjugate of Tetracyclin-AgNPs (12.5, 25, 50, and 100 µg/mL each) were tested for their antioxidant potential in a scavenging DPPH radical solution (0.02 g DPPH in 50 mL methanol). Ascorbic acid (10 µg/mL) was used as a positive control treatment. Firstly, a mixture that included the sample (750 µL) and DPPH, or ascorbic acid (750 µL), followed by storage at 37°C in darkness. A wavelength of 517 nm was adopted for the measurement of optical density (OD), whereas the Equation 1 below was utilized for the calculation of the antioxidant activity:

$$\text{Antioxidant activity \%} = \frac{(\text{OD Control} - \text{OD Sample})}{\text{OD Control}} \times 100 \quad (1)$$

OD control refers to the optical density of the control, and OD sample refers to the optical density of the sample.

Cytotoxicity analysis using 3-(4,5-Dimethylthiazol-2-yl)-2,5-Diphenyltetrazolium Bromide (MTT)

A breast cancer cell line MCF-7 (Michigan Cancer Foundation-7) was plated in 96-well microtiter plates (1× 104 cells/well) to evaluate their ability to stay viable in response to treatments (72 h) with AgNPs and the conjugate with the abovementioned concentrations, based on the MTT cell viability assay. The effect of treatment was tested by replacing the culture medium with 2 mg/mL of the MTT solution and incubating it (1.5 h, 37°C). Following the removal of MTT, dissolution of the produced formazan was achieved via the addition of DMSO (130 µL) and incubation (15 h, 37°C, with shaking) [23]. The ELISA kit reader and OD of 492 nm were utilized for reading absorbance. In contrast, inhibition rate as a parameter for testing the cytotoxic activity of triplicate treatments was extracted following the Equation 2 below:

$$\text{Inhibition rate (\%)} = \frac{(A - B)}{A} \times 100 \quad (2)$$

A and B = OD values for the control and the treatment, respectively.

2.9 Statistical analysis

The results were referred to as the mean ± SD of three replicates. Data were statistically analyzed utilizing the SPSS version 11.5 program. Differences were estimated by utilizing the Analysis of Variance (ANOVA) test. The significance of variations was demonstrated using the least significant difference (LSD) test.

3. Results and discussion

3.1 Characterization of conjugate Tetracycline –AgNPs

Generally, the biosynthesized nanoparticles are characterized by their size, shape, and dispersion [24]. Particle homogeneity, monodispersity with tiny sizes, and an extremely large surface area are among the required characteristics that would be important in several practical applications. The common techniques applied in this study for characterizing the bio-synthesized AgNPs are scanning electron microscopy (SEM) and energy dispersive spectroscopy (EDS). According to the previous study in [25], the UV absorbance showed the color shift of the tetracycline solution from pale yellow to greenish following the introduction of the Ag^+ ions, where the absorbance peak was at 390 nm.

Figure 1(A, B, and C) shows the appearance of silver nanoparticles using a scanning electron microscope (SEM), with an average particle size of 22.82 nm and a cubic shape. SEM is an important technology that uses radiation and electronic imaging to draw an image of the surfaces of materials, through which the shape of nanoparticles can be determined. EDX spectrum of silver NPs Figure 1D, exhibiting peaks corresponding to elemental silver, referred to in the literature as falling in the 3-3.5 keV range, and spectra for chlorine, oxygen, nitrogen, and potassium.

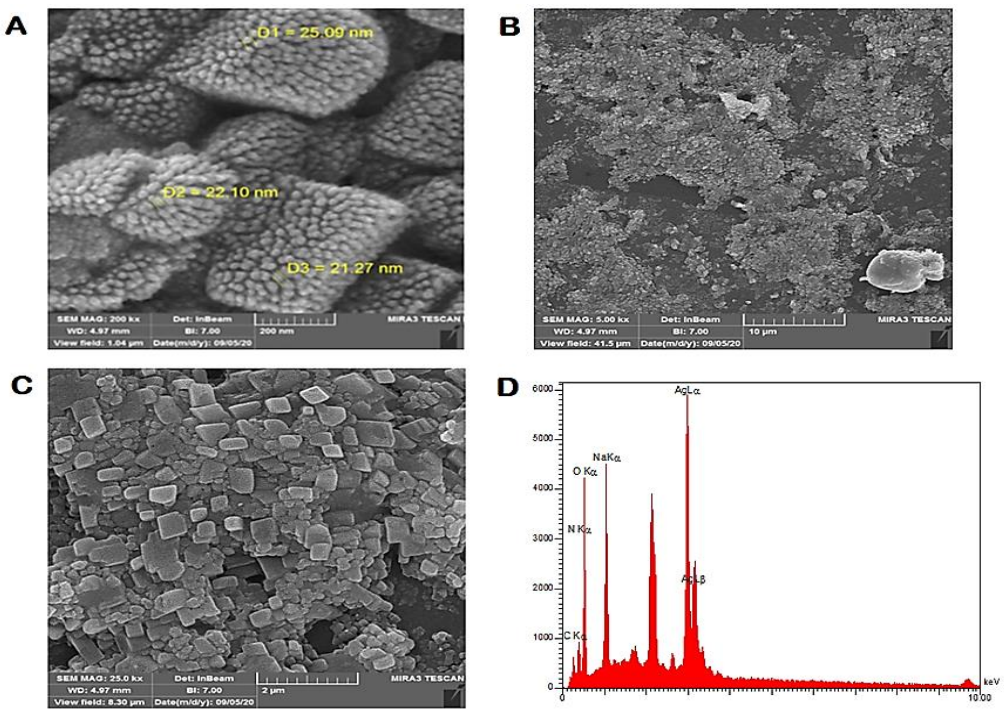

Figure 1: A-C refer to SEM images of AgNPs at different scale bars 200 nm, 10 µm , and 2 µm, respectively. D refers to the EDX spectrum of AgNPs

Other studies reported the synergistic effect of Tetracycline (TC) and AgNPs. TC-AgNPs yield was optimal when synthesized using the combination of silver nitrate, Tetracycline, and sodium hydroxide at a molar ratio of 1:6:24. Tetracycline works as a co-reducing and stabilizing agent [26]. AgNPs could be conjugated with various antibiotics such as Tetracycline (polykeptide), neomycin (aminoglycoside), and penicillin (β-lactam). The tetracycline- or neomycin-AgNPs conjugates could efficiently inhibit the bacteria's growth through the improved binding capacity of the Tetracycline- or neomycin-AgNPs conjugate with bacterial isolates [27].

3.2 Chromosomal Analysis

Results in Figure 2a-c and Table 1 reflect the behavior of peripheral blood lymphocytes (measured in terms of blastogenic index (BI), mitotic index (MI), and total chromosomal aberration (TCA) values in response to the treatment with pure AgNPs and their conjugate with Tetracycline. Figure 2A showed the microscopic image of noral metaphase, while images in figures 2B and C showed the dicentric and ring chromosomes , respectively. An apparent concentration-dependent increase in TCA values is observed, whereas BI and MI were subject to a significant reduction. These findings concur with earlier works on malignant cells regarding dose-dependent reductions in cell division rate, mitotic cell number, and the aggravation of chromosomal aberrations. Such responses are remarkably similar to the chemotherapy mechanism of action, which depends on inhibiting the mitotic spindle and, on the other hand, on inhibiting protein synthesis during the cell cycle [28–30]. Whether spontaneous or induced, Aberrations in chromosomes manifest as an altered structure or number of chromosomes [31]. Structure abnormalities might occur when the DNA is broken, its synthesis is inhibited, or its replication is based on altered strands. However, aberrations in the number of chromosomes, whether in polyploidy or aneuploidy, occur when they are abnormally segregated, either as a spontaneous behavior or in response to eugenic factors [32].

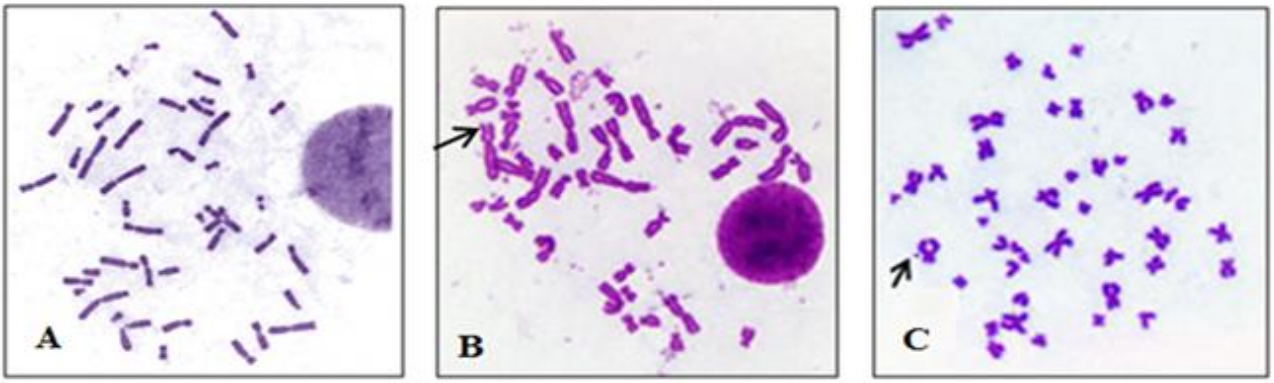

Figure 2: Chromosomal abberrations of peripheral blood lymphocytes. (A) normal metaphase, (B) Black arrow showing dicentric chromosome induced by Tetracycline –AgNPs at concentration of 100 µg/mL, (C) Black arrow showing ring chromosome induced by Tetracycline –AgNPs at concentration of 50 µg/mL. Magnification Power was 400X.

Table 1: Chromosomal aberrations n peripheral blood lymphocytes (PBLs) as a result of treatment with AgNPs, Tetracycline, and Tetracycline –AgNPs

AgNPs				Tetracycline				Tetracycline- AgNPs			
Conc.µg/mL	**BI**	**MI**	**TCA**	**Conc.µg/mL**	**BI**	**MI**	**TCA**	**Conc.µg/mL**	**BI**	**MI**	**TCA**
0.0	40.50	0.72	0.12	0.0	40.5	0.72	0.12	0.0	40.50	0.72	0.12
50	37.12	0.66	0.17	50	38.77	0.70	0.14	50	36.28	0.54	0.22
100	36.35	0.58	0.25	100	38.45	0.66	0.14	100	33.11	0.46	0.24
150	36.09	0.43	0.31	150	36.43	0.63	0.18	150	31.09	0.38	0.24
200	33.24	0.41	0.44	200	32.21	0.60	0.19	200	30.25	0.36	0.27
250	28.67	0.37	0.56	250	31.18	0.57	0.25	250	28.23	0.25	0.31
650.MTX	18.26	0.12	0.0								

3.3 Estimation of minimum inhibitory concentration

The MIC refers to the lowest concentration that causes the complete inhibition of bacterial growth. In the present work, this test was conducted using liquid culture media, involving both bacterial filtrate and silver nanoparticles, to determine the extent of the effect on the growth of the microorganism isolates by means of the turbidity test. It is noted from the results that almost all of the isolates recorded the minimum inhibitory concentration at 60%, while the minimum inhibitory concentration for two isolates (1 and 10) was 100%.

3.4 Growth Curve Test

A growth curve test was used to estimate the anti-bacterial activity of AgNPs (100 µg/mL) at zero time, 2 hours., and 6 hours. At exposure time zero, there was no significant effect on bacterial growth. However, the effect appears gradually after two hours of exposure and then 6 hours, which showed a significant effect in inhibiting bacterial growth in the isolates (C, E) or in the appearance of a small number of bacterial colonies as in the isolates (A, B, D, F, G, and H) (Figure 3). This is related

to the interactions of the AgNPs with the bacterial cell membrane. It is suggested that the sulfur and phosphorus-containing entities within the components of the cell walls are the favorite sites for the AgNPs, leading to bacterial cell breakdown and death. The AgNPs were observed to exhibit inhibition, and it was inferred that the AgNPs produce reactive oxygen species (ROS) in the nutrient broth, which led to the growth inhibition of bacteria. There is evidence that time contributes to the suppression and growth of bacteria. The growth time and lag phase for bacteria depend on nanoparticle characteristics and functional participation, including the conditions necessary for bacterial growth and development [33,34].

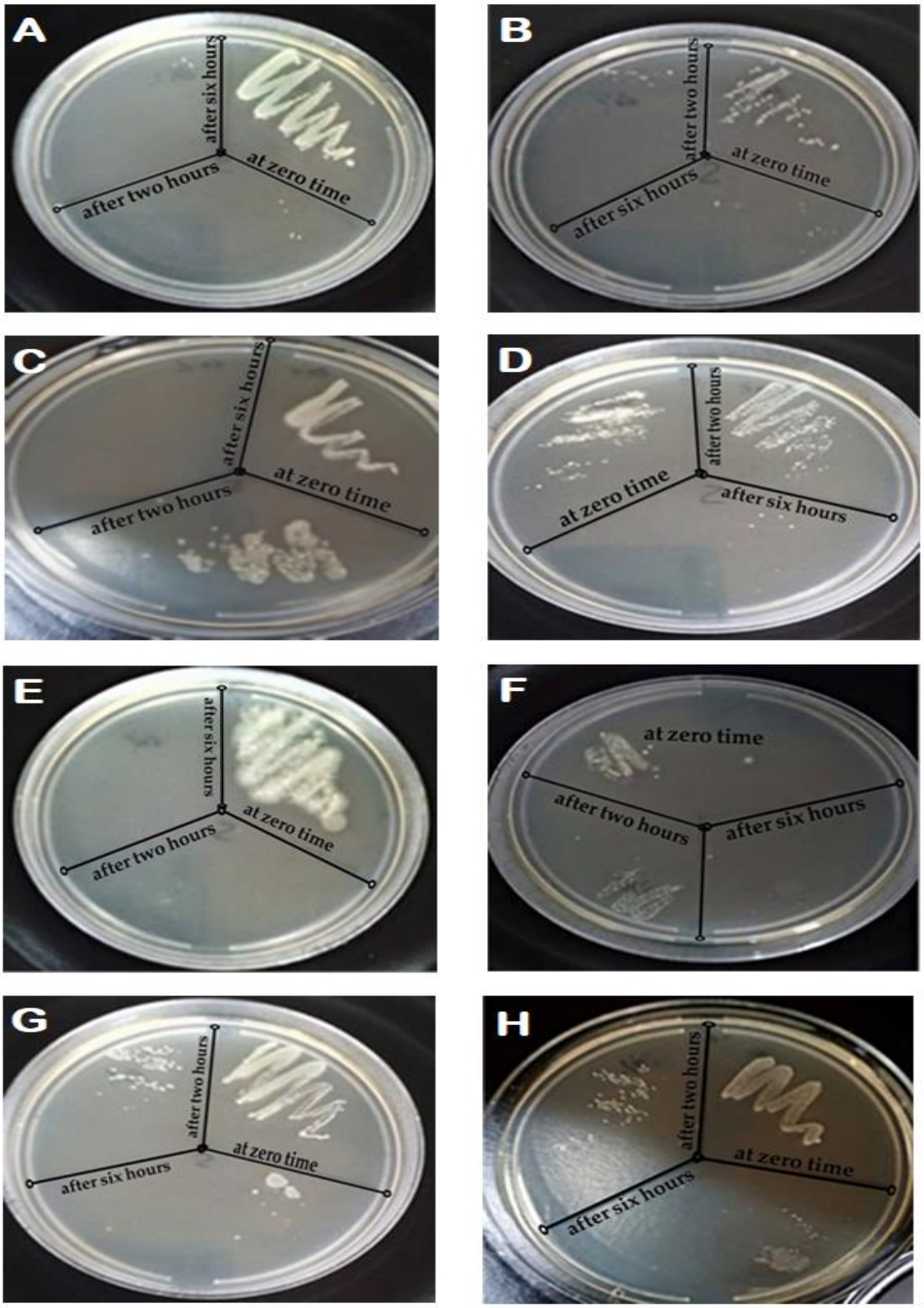

Figure 3: Growth curve assay of AgNPs against different P. aeruginosa isolates. A decrease in growth is observed after increasing the exposure time to AgNPs (zero time, 2 h, and 6 h). A. Isolate No.1, B. Isolate No.2, C. Isolate No.3, D. Isolate No.4, E. Isolate No.5,F. Isolate No.6, G. Isolate No.7, and H. Isolate No.8

3.5 Antioxidant potentials

DPPH shows high stability at room temperature while displaying a dark violet color after dissolving in an organic solvent. It has a strong absorption wavelength of 517 nm. When silver nanoparticles are added, the color shifts to yellow. Phenolic OH groups were reported to reduce DPPH (35–37). In the present work, the DPPH test revealed potential concentration-dependent scavenging impacts of sliver nanoparticles against free radicals. The results of the concentrations of the different treatments showed significant differences at a p-value ≤0.05. When conjugated to Tetracycline, this impact slightly increases compared with ascorbic acid at different concentrations (50, 100, and 150 µg/mL) Table 2. The DPPH (2,2-diphenyl-1-picryl-hydrazyl-hydrate) free radical method is an antioxidant assay based on electron transfer that produces a violet solution in ethanol. This free radical, stable at room temperature, is reduced by an antioxidant molecule, giving rise to a colorless ethanol solution. The use of the DPPH assay provides an easy and rapid way to evaluate antioxidants by spectrophotometry [10], so it can be useful to assess various products at a time.

Table 2: The antioxidant effects using the DPPH method for different concentrations of Tetracycline-AgNPs

Tetracycline- AgNPs			Ascorbic Acid		
Conc. µg/mL	**Abs**	**AA%#**	**Conc. µg/mL**	**Abs**	**AA%#**
0.0	0.280±0.04	0.0	0.0	0.280±0.04	0.0
50	0.175±0.02	37.50 ^{Aa}	50	0.167±0.01	40.35 ^{Aa}
100	0.163±0.03	41.79 ^{Ba}	100	0.122±0.01	56.42 ^{Bb}
150	0.141±0.02	49.65 ^{Ca}	150	0.097±0.01	65.35 ^{Cb}

#AA%=Percentage of antioxidant activity; Abs: Absorbance
Different capital case letters: Significant difference (P ≤ 0.05) between means of columns.
Different lowercase letters: Significant difference (P ≤ 0.05) between means of rows.

3.6 Anti-cancer activity of nanoparticles

The influence of silver nanoparticles on the growth of the MCF-7 cell line is illustrated in Figure 4. As shown in Figure 4A, treatment with tetracycline-AgNPs at concentrations of 26.5 and 100 µg/mL showed a concentration-dependent decrease in the number of colonies of MCF-7 as compared to those of non-treated cells. The viability of tumor cells after 24 h of incubation with 50 µg/mL was highly affected (60%). Similar toxicity effects were obtained with the high concentration, but the effect was more potent (85%) than that observed in the previous one Figure 4A. Figure 4B showed the microscopic image of MCF-7 cell line before treatment with AgNPs, while figure 4C showed the microscopic image of MCF-7 cells after treatment with AgNPs at concentrations 50 µg/mL which rvealed a decrease in number of colonies of MCF-7 as compared to those of nontreated cells Figure 4B.

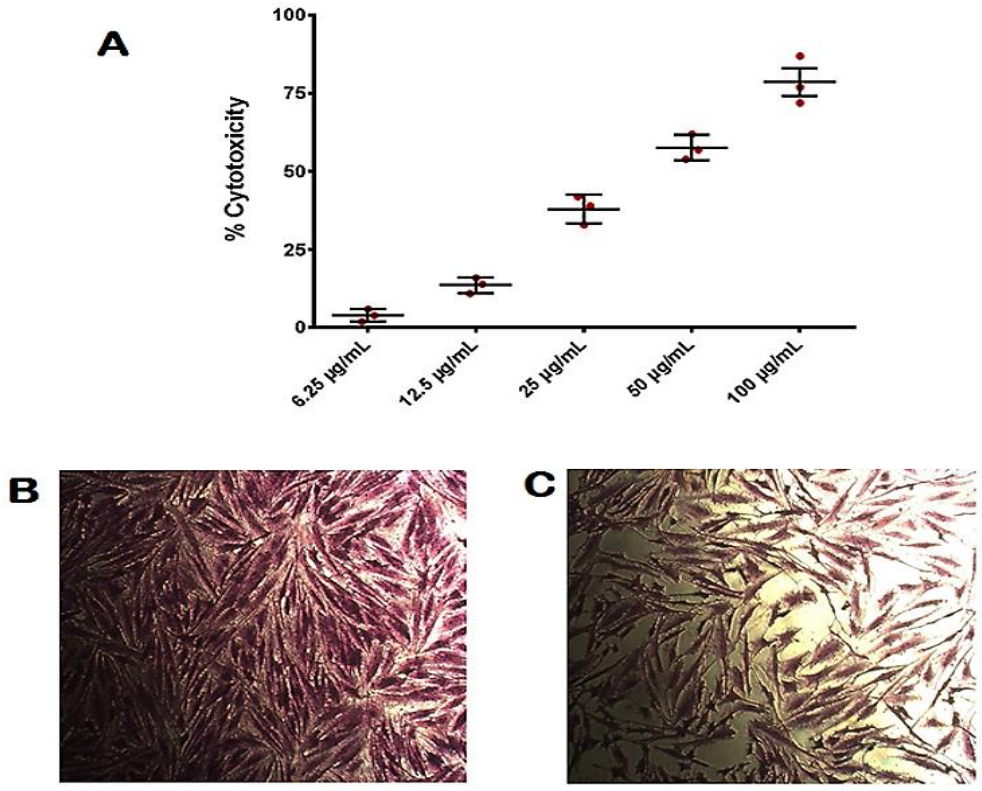

Figure 4: Cytotoxic effect of AgNPs on MCF-7 cell line, A: Percentage of cytotoxicity against MCF-7 cells B: before treatment with AgNPs, While C. after treatment with AgNPs

Cancer takes its rank as being among the most common fatal factors worldwide. Further investigations are required to discover the capability of the natural products of different plants to overcome the emerging issue of resistance to anti-cancer drugs. In recent times, plants, herbs, and materials introduced by traditional medicine have been clearly appreciated as a major pool for producing chemical drugs to prevent malignancy and various other health applications. Thus, decisions about their potential and diverse usages need to be built on an extensive information base covering their properties in terms of benefits and risks. For example, spices are known to be the source of active components found in dietary phytochemicals. The findings of the present work could infer that the NPs, which have been under extensive research during the last decade, are of great value as nature-derived chemicals with strong actions against microorganisms and free radicals. Nevertheless, further investigation is essential to better identify the compounds with biological activity, including in vivo studies using suitable animal species [20]. The toxic, antitumor effect of the prepared nanoparticles NPs against MCF-7 cells was investigated by examining their capability of inhibiting proliferation, demonstrating highly significant effects, as shown in Figure 4. An indication of such an impact was extracted from their clear potential to inhibit the proliferation of the targeted cells in a dose-dependent manner. Recent studies indicated that treating cancer cells with NPs for 72 hours helped in the emergence of a noticeable decrease in the reproduction capacity of these cells. Other findings indicated that these particles confer a selective induction of cell death and growth inhibition on THP-1 and AMJ-13 cells [38].

4. Conclusion

This work established that using the chemical reduction approach to synthesize AgNPs confers them with relatively higher stability in terms of physiochemical characteristics. The conjugate between these particles and Tetracycline resulted in a product with potent antibiotic, antitumor, and anti-free radical properties. The widespread concern about antibiotic-resistant microbes promotes research in discovering new antibiotic compounds and the pharmaceutical development of antibiotic drugs. AgNPs have been proven to have anti-bacterial activity and are used in various products, such as cosmetics, medical products, and anti-microbial dressings. The article provides a state-of-the-art review of the physicochemical factors that affect its bactericidal activity and mechanism of action. It highlights the synergistic anti-bacterial activity of antibiotic-AgNP conjugates against drug-resistant bacteria. Studies reported that AgNPs physicochemical parameters that affect the anti-microbial activity of the particles are size, shape, surface charge, concentration, and colloidal state. The anti-bacterial activity of these nanoparticles works through direct contact with the bacteria's cell surface and membrane, and penetration through the bacteria's cell leads to intracellular cell damage, cell toxicity, oxidative stress, and signal transduction pathway alteration. These activities were enhanced when the AgNPs were conjugated with antibiotics. Information regarding the effects of AgNPs at a cellular level is essential to further determining the dosage and safety profile. In addition, knowledge about the characteristics of AgNPs in biological systems and their synergism with antibiotics will offer essential information in developing nanomaterial technologies to prevent and treat infections caused by pathogenic bacteria. That is why suitable approaches for their usage must be premeditated and fostered to relegate the emergence of resistant strains.

Acknowledgment

The authors highly appreciate the support provided by the Department of Applied Science Laboratories, University of Technology, Baghdad, Iraq. The research has not received funding secured from the author’s resources.

Author contributions

Conceptualization, N. Hussein, Z. Zghair, R. Hussein, H. Mohammed, A. Hameed, A. Abduljabar, B. Hasoon and Gh. Sulaiman; investigation, N. Hussein, Z. Zghair, R. Hussein, A. Hameed, A. Abduljabar and B. Hasoon.; methodology N. Hussein, Z. Zghair, R. Hussein, A. Hameed, A. Abduljabar and B. Hasoon; software, H. Mohammed.; writing—original draft preparation, N. Hussein, Z. Zghair, R. Hussein, A. Hameed, A. Abduljabar and B. Hasoon.; writing—review and editing, N. Hussein, Z. Zghair, R. Hussein, A. Hameed, A. Abduljabar and B. Hasoon. All authors have read and agreed to the published version of the manuscript.

Funding

This research received no specific grant from any funding agency in the public, commercial, or not-for-profit sectors.

Data availability statement

The data that support the findings of this study are available on request from the corresponding author.

Conflicts of interest

The authors declare that there is no conflict of interest.

References

[1] M. Nelson , S. Levy , The history of the tetracyclines, Ann N Y Acad Sci., 1241 (2011) 17–32. https://doi.org/10.1111/j.1749-6632.2011.06354.x

[2] D. Fuoco, Classification framework and chemical biology of tetracycline-structure-based drugs, Antibiotics, 1 (2012) 1–13. https://doi.org/10.3390%2Fantibiotics1010001

[3] H. Mohammed, M. Amin, G . Zayed, Y . Hassan, M . El-Mokhtar, M. Saddik , In vitro and in vivo synergistic wound healing and anti-methicillin-resistant Staphylococcus aureus (MRSA) evaluation of liquorice-decorated silver nanoparticles, J Antibiot ., 76 (2023) 291–300. https://doi.org/10.1038/s41429-023-00603-4

[4] D. Ibraheem, N. Hussein, G. Sulaiman, H. Mohammed, R. Khan, O. Al Rugaie, Ciprofloxacin-Loaded Silver Nanoparticles as Potent Nano-Antibiotics against Resistant Pathogenic Bacteria, Nanomaterials, 12 (2022) 2808. https://doi.org/10.3390/nano12162808

[5] H. Al-Shmgani, M. Ashij, K. Khalil, H. Mohammed , Synthesis and Characterization of Proteolytic Enzyme Loaded on Silver Nanoparticles, J. Pure. Appl . Sci., 37 (2024) 43–53. DOI: https://doi.org/10.30526/37.1.3300

[6] R. Prasad, K . Elango, D . Damayanthi, J. Saranya , Formulation and evaluation of azathioprine loaded silver nanopartilces for the treatment of rheumatoid arthritis, 3 (2013) 28–32.

[7] B . Buszewski, K .Rafiſska, P. Pomastowski, J .Walczak, A. Rogowska, Novel aspects of silver nanoparticles functionalizationm, Colloidsm, Surf. A: Physicochem. Eng. Asp., 506 (2016) 170–178. http://dx.doi.org/10.1016/j.colsurfa.2016.05.058

[8] P . AshaRani, G . Mun, M. Hande, S.Valiyaveettilm, Cytotoxicity and genotoxicity of silver nanoparticles in human cells, ACS Nano., 3 (2009) 279–290. https://doi.org/10.1021/nn800596w

[9] M. Hajipour, K. Fromm, A. Ashkarran, D. Aberasturi, I. Larramendi, T . Rojo, et al, Anti-bacterial properties of nanoparticles, Trends. Biotechnol., 30 (2012) 499–511. https://doi.org/10.1016/j.tibtech.2012.06.004

[10] T. Dakal, A . Kumar, R. Majumdar, V. Yadav, Mechanistic basis of anti-microbial actions of silver nanoparticles, Front Microbiol, 7 (2016) 231711. https://doi.org/10.3389%2Ffmicb.2016.01831

[11] S . Ahmed, M . Ahmad, B. Swami, S. Ikram, A review on plants extract mediated synthesis of silver nanoparticles for anti-microbial applications: A green expertise, J. Adv. Res., 7 (2016) 17–28. https://doi.org/10.1016%2Fj.jare.2015.02.007

[12] N . Durán, M. Durán, M. Jesus, A. Seabra, W. Fávaro, G. Nakazato, Silver nanoparticles: A new view on mechanistic aspects on anti-microbial activity, Nanomed. Nanotechnol. Biol. Med., 12 (2016) 789–799. https://doi.org/10.1016/j.nano.2015.11.016

[13] S. Anuj, H. Gajera, D. Hirpara, B. Golakiya , Bactericidal assessment of nano-silver on emerging and re-emerging human pathogens, J .Trace. Elem. Med. Biol., 51 (2019) 219–225. https://doi.org/10.1016/j.jtemb.2018.04.028

[14] A. Jabbar, N. Hussian, H. Mohammed, A . Aljarbou, N .Akhtar, R. Khan , Combined Anti-Bacterial Actions of Lincomycin and Freshly Prepared Silver Nanoparticles: Overcoming the Resistance to Antibiotics and Enhancement of the Bioactivity, Antibiotics,11 (2022) 1791. https://doi.org/10.3390/antibiotics11121791

[15] K. Qureshi, A. Bholay, P. Rai, H. Mohammed, R. Khan, F . Azam , at al, Isolation, characterization, anti-MRSA evaluation, and in-silico multi-target anti-microbial validations of actinomycin X2 and actinomycin D produced by novel Streptomyces smyrnaeus, Sci. Rep., 11 (2021) 1–21. https://doi.org/10.1038/s41598-021-93285-7

[16] K . Lee, E. Silva, D. Mooney , Growth factor delivery-based tissue engineering: general approaches and a review of recent developments, J . R. Soc. Interface., 8 (2011) 153–70. https://doi.org/10.1098/rsif.2010.0223

[17] S. Neamah, S .Albukhaty, I. Falih, Y. Dewir, H. Mahood, Biosynthesis of Zinc Oxide Nanoparticles Using Capparis spinosa L. Fruit Extract: Characterization, Biocompatibility, and Antioxidant Activity, Appl Sci., 13 (2023) 6604. https://doi.org/10.3390/app13116604

[18] I . Pinzaru, D .Coricovac, C. Dehelean, E. Moacă, M. Mioc, F. Baderca, et al, Stable PEG-coated silver nanoparticles–A comprehensive toxicological profile, Food Chem Toxicol., 111 (2018) 546–556. https://doi.org/10.1016/j.fct.2017.11.051

[19] D . Dehghan, M. Ramandi, R. Taheri , Investigation of Synergism of Silver Nanoparticle and Erythromycin Inhibition and Detection of Exotoxin-A Gene in Pseudomonas aeruginosa Isolated from Burn Wounds Secretion, J . Med .Microbiol., 14 (2020) 379–89. http://dx.doi.org/10.30699/ijmm.14.4.379

[20] A. Hameed, N. Hussein, Detection of antibiofilm formation by sliver nanoparticles created by tetracycline antibiotic, J. Phys. Conf. Ser., 1879 (2021) 022035. http://dx.doi.org/10.1088/1742-6596/1879/2/022035

[21] A. Chahardehi, D . Ibrahim, S. Sulaiman, L. Mousavi , Time-kill study of ethyl acetate extract of stinging nettle on bacillus subtilis subsp. spizizenii ATCC CRM-6633 Strain NRS 231, Annu. Res. Rev. Biol., 6 (2014) 33–40.

[22] Verma RS, Babu A. Human chromosomes: manual of basic techniques. 1989.

[23] H. Muslim , Detection of the anti-bacterial activity of AgNPs biosynthesized by Pseudomonas aeruginosa, J. Agric. Sci., 2 (2019). https://doi.org/10.36103/ijas.v2i50.661

[24] J . Jiang, G . Oberdörster, P . Biswas, J. Characterization of size, surface charge, and agglomeration state of nanoparticle disp ersions for toxicological studies, J. Nanopart. Res.,11 (2009) 77–89. http://dx.doi.org/10.1007/s11051-008-9446-4

[25] B. Aggarwal, S. Shishodiam, Molecular targets of dietary agents for prevention and therapy of cancer, Biochem Pharmacol, 71 (2006) 1397–421 . http://dx.doi.org/1016/j.bcp.2006.02.009. Epub 2006 Feb 23

[26] R . Thomas, A. Nair, S . Kr, J. Mathew, R. Ek, Anti-bacterial activity and synergistic effect of biosynthesized AgNPs with antibiotics against multidrug-resistant biofilm-forming coagulase-negative staphylococci isolated from clinical samples, Appl. Biochem. Biotechnol., 173 (2014) 449–60. doi: 10.1007/s12010-014-0852-z. Epub 2014 Apr 4

[27] D. McShan, Y . Zhang, H . Deng, P. Ray, H .Yu, Synergistic anti-bacterial effect of silver nanoparticles combined with ineffective antibiotics on drug resistant Salmonella typhimurium DT104, J .Environ. Sci .Heal Part C, 33 (2015) 369 – 384. https://doi.org/10.1080/10590501.2015.1055165

[28] R. Hikmet, N. Hussein , Mycosynthesis of silver nanoparticles by Candida albicans yeast and its biological applications, Arch. Razi. Inst.,76 (2021) 857– 869. https://doi.org/10.22092/ari.2021.355935.1741

[29] T .Ong, J. Nath, Cytogenetic effects of vincristine sulfate and ethylene dibromide in human peripheral lymphocytes: micronucleus analysis, Environ. Mol .Mutagen., 20 (1992) 117–26. https://doi.org/10.1002/em.2850200207

[30] M. Fahmy, E. Hassan, A. Farghaly, Z. Hassan , Genotoxicity, DNA damage and sperm defects induced by vinblastine, Mol .Biol. Rep., 50(2023)1059– 1068. https://doi.org/10.1007/s11033-022-08061-1

[31] W. Jiang, Y. Lu, Z . Chen, S. Chen, M .Zhang, L .Jin, et al. Studying the genotoxicity of vincristine on human lymphocytes using comet assay, micronucleus assay and TCR gene mutation test in vitro, Toxicology, 252 (2008) 113–117. https://doi.org/10.1016/j.tox.2008.07.057

[32] Gardner R, Sutherland G, Shaffer G. Chromosome abnormalities and genetic counseling. OUP USA; 2012.

[33] R. Albertini, D .Anderson, G. Douglas, L. Hagmar, K .Hemminki, F . Merlo, et al. IPCS guidelines for the monitoring of genotoxic effects of carcinogens in humans, Mutat. Res. Rev. Mutat. Res., 463 (2000) 111–172. https://doi.org/10.1016/s1383-5742(00)00049-1

[34] S .Sharaf, H. Abbas, T. Ismaeil , Characterization of spirugenic iron oxide nanoparticles and their anti-bacterial activity against multidrug-resistant Helicobacter pylori, J .Phycol., 20 (2019)1–28. https://doi.org/10.21608/egyjs.2019.116018

[35] Z. Kashmiri, S. Mankar , Free radicals and oxidative stress in bacteria, Int. J .Curr. Microbiol. Appl .Sci., 3 (2014) 34 – 40.

[36] G . Sulaiman, F. Elshibani , at al. The Flavonoid Molecule of Antioxidant Interest, Chemistry Select, 8 (2023)1–15. https://doi.org/10.1002/slct.202303306

[37] H. Mohammed, R .Khan , Anthocyanins: Traditional Uses, Structural and Functional Variations, Approaches to Increase Yields and Products' Quality, Hepatoprotection, Liver Longevity, and Commercial Products, Int .J. Mol. Sci., 23 (2022) 2149. https://doi.org/10.3390/ijms23042149

[38] D . Huang, B . Ou, R . Prior , The chemistry behind antioxidant capacity assays. J. Agric. Food. Chem., 53 (2005)1841–1856. https://doi.org/10.1021/jf030723c